N87-26442

ITO/InP Solar Cells: A Comparison of Devices Fabricated by Ion-Beam and RF Sputtering of the ITO

T.J. Coutts
Solar Energy Research Institute
Golden, Colorado

This work has been performed with a view to elucidating the behavior of ITO/InP solar cells prepared by rf and ion-beam sputtering. It is found that using rf sputter deposition of the ITO always leads to more efficient devices than ion-beam (IB) sputter deposition. An important aspect of the former technique is the exposure of the single crystal p-InP substrates to a very low power plasma, prior to deposition. Substrates treated in this manner have also been used for ion-beam deposition of the ITO. In this case the cells behave very similarly to the rf deposited cells, thus suggesting that the low power plasma exposure (LPPE) is the crucial process step.

Detailed analysis of the quantum efficiency of the cells shows that the LPPE causes the formation of a very thin type-converted surface layer on the p-type substrate, leading to a buried homojunction. These cells always had a much larger V_{oc} than the IB only cells, although the latter had a slightly larger J_{sc}. The largest J_{sc} achieved for the IB cells (of area nearly 1 cm^2) is 27.7 mA cm^{-2} (total area, 28°C, 100mW cm^{-2}, SERI/NASA direct normal spectrum). This is equivalent to 33.5 mA cm^{-2} (total area 28°C, 137.2 mW cm^{-2}, AMO WRRL-1985) which is, at the time of writing, the largest yet reported for any InP based cell. However the largest V_{oc} we have achieved is only 802 mV (28° C, for one of the rf cells), which is much less than should be expected for InP.

INTRODUCTION

Although the suitability of InP for solar cells has long been recognized, it has largely been ignored by the research community (principally because of its relatively high materials cost). In thin film form, where the cost considerations do not apply, it has also been discounted as an absorber for terrestrial solar cells because of unsolved problems of severe grain boundary recombination. The latter remains an outstanding question; why should grain boundary recombination be so severe when surface recombination is so minimal a problem? Hence, although InP has all the properties required for the fabrication of efficient solar cells (Eg=1.35 eV, direct band-gap and large absorption coefficient, low surface recombination velocity, and acceptably long minority carrier diffusion length), it has only been investigated by a relatively small number of research groups (1-5).

In recent years, however, this situation has begun to change, largely because of the extraordinary radiation resistance and annealing properties which InP exhibits (6-8). This has stimulated an appreciation of its potential for space applications which in turn may cause renewed interest in thin film cells for terrestrial application.

p-InP absorbers have been used with a variety of window-layers; e.g., with CdS (1), ZnO (9) and indium tin oxide (ITO) (2) being the most commonly studied. On the basis of elementary heterojunction design considerations, (lattice match, electron affinity match, window layer transmittance etc), one would expect the CdS/InP combination to have the highest efficiency of these three, whereas in practice it is the ITO/InP cell which has this record (2). The reasons for this somewhat unexpected

behavior have been the subject of considerable debate, and part of the objective of this paper will be the elucidation of ITO/InP junctions for cells in which the ITO has been deposited by either rf or ion-beam (IB) sputtering. This has established that the former are actually extremely shallow buried homojunctions, whereas the latter are more like true heterojunctions. However, it is concluded that in neither case will efficiencies approaching theoretical values be achieved. Rather, further advances will depend on optimizing the performance of n^+-p-p^+ cells, probably grown by OMCVD on the p^+ substrate.

EXPERIMENTAL

In this work, single crystal p-type InP has been used. The orientation was <100>; the crystals were zinc doped and two impurity concentrations were investigated; these being $N_A-N_D = 3x10^{16}$ cm^{-3} (purchased from Crysta Comm Inc.) and $3x10^{15}$ cm^{-3} (MCP Ltd.)

Device fabrication followed the sequence below:

i) Contact formation - after cleaving the as delivered wafer into substrates of approximately 1 cm^2 in area, the latter were chemo-mechanically polished with 0.25 μm diameter Al_2O_3 grit and 0.05 v/o Br: methanol. After this procedure the surface was examined ellipsometrically to check for residual roughness or contamination. Generally, it was found that the surface gave ellipsometric data close to that predicted for an ideal InP surface. Metal contacts were then deposited. In the work reported here, the metallization was 200Å of Zn (deposited by rf sputtering) followed by 2000Å of Au (deposited by thermal evaporation). The metallized substrate was then annealed in flowing forming gas for about one minute at a temperature of approximately 425°C. Contacts made this way tended to be somewhat variable and alternative systems based on Au:Be and Ni/Au:Be are now being studied.

ii) Active surface cleaning - because InP selectively loses phosphorus at quite low temperatures, it was always necessary to re-etch the front surface after contact formation. This was done in exactly the same manner as described above.

iii) Deposition of ITO - the ITO was deposited either by rf sputtering or by ion-beam sputtering. We have previously shown that exposure of the substrates to an extremely low power rf plasma, prior to deposition of the ITO, led to a great enhancement of device performance (10). To elucidate the effects of the low power plasma exposure (LPPE) we have made three types of cell. Type 1 cells were made entirely in the rf system. The ITO target was first sputter cleaned at full power for about thirty minutes, with the InP substrates protected by a shutter. The power was then reduced to a level at which no deposition was registered by a quartz crystal monitor. The shutter was then opened and the substrates subjected to LPPE for a pre-determined period. After this, the power was increased to give a rate of deposition of about 0.3-0.4Å s^{-1} and a film of ITO about 650Å grown. Type 2 cells were also subjected to the LPPE but after this were removed from the rf system and transferred to the ion-beam system for deposition of the ITO. Again, 650Å of ITO was used. Type 3 cells were not subjected to LPPE and the ITO was deposited by ion-beam sputtering.

iv) Gridding - was carried out using the temporary grids described elsewhere (11). The grids were electroformed from copper and were Au plated. They were held in close contact with the ITO using Scotch Tape. Although almost laughable in its lack of sophistication, this technique has proved remarkably successful as evidenced by the high device efficiencies achieved. However, the shadowing loss of these grids was 8-9% whereas recent calculations have shown that optimal grids would have shadow

losses of about 3%. More recent work on the electroplated grids will be published later.

v) Device characterization - the J/V, C/V and quantum efficiency of all the cells were measured. For efficiency measurements, standarized conditions of intensity, spectral content and temperature were used (total area, 28°C, 100mW cm^{-2}, SERI/NASA, direct normal spectrum). The C/V measurements were made using a Hewlett-Packard LCR bridge (Type 4274 A) at a frequency of 100 kHz. Reverse biases up to 10V have been used but were generally restricted to about 4V. The quantum efficiency measurements were made as a function of reverse voltage bias and light bias. It is the analysis of these measurements which will form the basis for most of the subsequent discussion.

RESULTS

The performance characteristics of all sixteen cells are summarized in tables 1 and 2; with the current/voltage characteristics of cells rf4 and IB1 (60 mins. LPPE, rf sputtered ITO; 0 mins. LPPE, IB sputtered ITO; respectively) being shown in Fig. 1. Cell rf4 had a value of J_{sc} = 27.7 mA cm^{-2} for the measurement conditions defined above. Using the spectral response of this cell, it was calculated that the AMO value of J_{sc} would be 33.5 mA cm^{-2} (using the total area of the cell = 0.981 cm^2, 28°C, 137.2 $mWcm^{-2}$ AMO WRRL - 1985). Since these cells had a grid shadow loss of about 8.5%, the actual active area current = 36.6 mA cm^{-2} which is to be compared with the theoretical maximum of 41.82 $mAcm^{-2}$.

The quantum efficiencies for cells rf1-4 are shown in Fig. 2 from which the completely systematic improvement with increasing LPPE is evident. This, of course is reflected in J_{sc}. Cells rf5-8 showed similar behavior although the optimum LPPE was 30 mins.

It should also be noted that all the rf series cells had $V_{oc} \geq 746$ mV whereas only those cells which had been rf plasma exposed, in the IB series, had relatively large V_{oc}. Cells IB1 and IB5 which had not been plasma exposed had high currents but low voltages. (Cell IB2 should not be included in this analysis since it was accidentally exposed to the ion-beam prior to deposition of the ITO). These key differences in the behavior of the two types of cell provide much information and they will be discussed later.

Plots of $1/C^2$ - V were also made and an illustrative example is shown in Fig. 3. The important feature to note here is that the IB cell gave nearly perfect linearity for the entire range of biases used whereas the rf cell showed a discontinuity. This behavior was typical.

DISCUSSION

It has previously been suggested that rf sputter deposition of any window layer material onto p-InP causes type conversion of the surface (9) and, indeed, direct evidence of phosphorus depletion has been obtained (12). In addition, "mixing" at the interface has been observed (13), as has the in-diffusion of tin (14), and the out-diffusion of dopants (15). Hence there are several processes known to take place at, or near, the interface which could radically influence the behavior of the cells. We believe that the larger values of V_{oc} and the lower values of J_{sc} are clear indications that the rf fabricated cells are buried homojunctions, while the IB cells, with their slightly larger J_{sc} (for the unexposed devices) and much lower V_{oc}, are probably heterojunctions.

In the absence of interface recombination, the internal quantum efficiency of a homojunction with disimilar diffusion lengths in the p- and n-regions, is

$$\eta_{int} = \left(\frac{e^{-\alpha d}}{1-\alpha L_p}\right) - \left(\frac{\alpha L_p e^{-d/L_p}}{1-\alpha L_p}\right) - \left(\frac{e^{-\alpha(d+W)}}{1+\alpha L_n}\right) \quad (1)$$

where α is the optical absorption coefficient, L_n and L_p are the minority carrier diffusion lengths, d is the thickness of the type-converted surface region, and W is the width of the space charge region. At the short wave-end of the spectrum, where α is large, it is straightforward to show that

$$\eta_{int} = \exp(-\alpha d) \quad (2)$$

provided that L_p is very small; i.e., that the surface is essentially "dead". From the measured reflectance spectrum of the cells we can calculate η_{int}, and these data can then be plotted in the form of $\ell n\ \eta_{int}$ ~α to obtain the thickness of the dead-layer. An example of such a plot is shown in Fig. 4 and it should be stressed that this technique worked only for the plasma exposed cells. IB1 and IB5 did not exhibit this behavior. In Fig. 5 we show the variation of the dead-layer thickness with plasma exposure time for the eight rf series cells. The striking feature is that the dead-layer decreases in thickness; monotonically for the more lightly doped material, and passing through a minimum for the 3×10^{16} cm^{-3} material (the latter observation is also reflected in the variation of J_{sc} with LPPE duration). The fact that cells rf1 and rf5 with no LPPE have the thickest dead-layers, and have relatively large voltages, whereas cells IB and IB5 (also without LPPE) have no dead-layer and have relatively low voltages, implies that most of the type-conversion mechanism takes place in the initial stages of the ITO deposition by rf sputtering. Hence the LPPE must somehow lessen the damaging effects of deposition, and we speculate that it somehow causes migration of acceptor impurities to the surface (as observed by SIMS (14)) which therefore makes the subsequent type-conversion of that region more difficult. The out-diffusion of acceptor species would also create a very lightly doped, graded sub-surface region which would have the effect of widening the space charge. This would lead to improved quantum efficiencies at all wavelengths.

To check this model we have examined the variation of dead-layer thickness with substrate impurity concentration. These data are shown in Fig. 6 for a fixed duration LPPE. As predicted by the model, the dead-layer thickness decreases as the impurity content of the substrates increase.

Finally, we have also made measurements of the dead-layer thickness as a function of reverse bias for one of the rf cells. The data are shown in Fig. 7 where d is plotted against W; the latter having been obtained from measurement of capacitance as a function of reverse bias. We interpret the decrease of d with increasing W as being due to the expansion of the space charge toward the surface of the type-converted region (i.e., toward the ITO interface) as well as into the p-type bulk. This, of course, also supports the homojunction model. If we assume that the change in the space charge width is proportional to the square root of the impurity concentration, then

$$\frac{\Delta d}{\Delta W} \approx \frac{|N_A - N_D|_p}{|N_D - N_A|_n}^{1/2} \quad (3)$$

For a reverse bias of 10V, $\Delta d \approx 80$ Å, $\Delta W \approx 0.5$ μm, and $|N_A-N_D|_p = 3\times10^{16}$ cm^{-3}. We have $|N_D-N_A|_n = 1\times10^{20}$ cm^{-3}. Dautremont-Smith et al have shown that deposition by rf sputtering of SiO_2 onto p-InP causes considerable disruption of the surface. Measured in terms of an areal density, the damage was of the order of 10^{15} cm^{-2}. If expressed in terms of a volume density, this number would be about 10^{22} cm^{-3} which could, therefore, be the donor concentration in the surface region. However, the net donor concentration, $|N_D-N_A|$, will actually be substantially less than this, due to compensation by out-diffusion acceptor species, and a value around 10^{20}cm^{-3} would not seem unreasonable. hence, it is believed that the benefits of the LPPE are due to making the surface strongly p^+ before being compensated to n^+ by damage due to the actual deposition of the ITO. This is more consistent with all the experimental observations than the in-diffusion of tin, suggested earlier (14,15), and is consistent with the recent observations of Olego et al (16). Hence, to summarize, the cells fabricated entirely in the rf system are essentially n^{++}(ITO)$|n^+$(InP)$|$p(InP), while those made using LPPE plus IB sputtering are possibly n^{++}(ITO)$|p^+$(InP)$|$p(InP). The IB only cells would be expected to be n^{++}(ITO)$|$p(InP). It is believed that this model explains all our observations.

CONCLUSIONS

This work has shown that ITO/InP cells, in which the ITO has been deposited by rf sputtering, are actually very shallow buried homojunctions. The influence of LPPE is to increase J_{sc}, particularly for the more lightly doped material. Substrates which were first plasma exposed on then had ITO deposited by IB sputtering, behaved similarly to the rf series cells. Conversely, IB sputtering and no LPPE, led to poor voltages and the largest J_{sc} of all. We conclude that these are actually true heterojunctions.

Measurement of the dead-layer thickness of the rf cells as a function of voltage has enabled us to estimate the effective concentration of donors in the type-converted surface layer. This is roughly in accordance with the damage estimates by Rutherford backscattering spectroscopy. Although we have made cells with efficiencies even higher than these (16.2% (2)), further substantial improvement is unlikely. The damage mechanism must inherently limit V_{oc} and the fill-factor and therefore we believe that realization of the full potential of this material will ultimately depend on optimization of OMCVD grown n^+-p-p^+ structures recently reported (7).

REFERENCES

1. S. Wagner, J.L. Shay, K.J. Bachmann, and E. Buehler, Appl. Phys. Letts., 26, 229 (1975).

2. T.J. Coutts and S. Naseem, Appl. Phys. Lett., 46, 164 (1985).

3. L. Gouskov, H. Luquet, J. Esta and C. Gril, Solar Cells, 5, 51 (1981).

4. T.L. Chu, S.S. Chu, C.L. Lin, C.T. Chang, Y.C. Tzeng and A.B. Kuper, Proceedings of the 14th IEEE PV Spec. Conf., San Diego, Jan. 7-10 (1980), p. 661.

5. N.G. Dhere, R.G. Dhere and H.R. Moutinho, Proceedings of the 18th IEEE PV Spec. Conf., Las Vegas, Oct. 21-25, (1985), p. 1423.

6. A. Yamamoto, M. Yamaguchi and C. Uemura, Appl. Phys. Lett., 44 611, (1984).

7. M. Yamaguchi, A. Yamamoto, Y. Itoh, and C. Uemura, Proceedings of the 2nd International Photovoltaic Science and Engineering Conference, Beijing, Aug. 19-22, (1986), p. 573.

8. I. Weinberg, C.K. Swartz and R.E. Hart, Proceedings of the 18th IEEE PV Spec. Conf., Las Vegas, Oct. 21-25 (1985), p. 1722.

9. M.J. Tsai, A.L. Fahrenbruch and R.H. Bube, J. Appl. Phys., 51, 2696, (1980).

10. T.J. Coutts and N.M. Pearsall, Proceedings of the IEE Meeting on Plasma Deposition Processes, London, (1982).

11. N.M. Pearsall, Ph.D. Thesis, Cranfield Institute of Technology, Cranfield, Bedfordshire, England, (1982).

12. W.C. Dautremont-Smith and L.C. Feldman, J. Vac. Sci. Technol. A 3, 873 (1985).

13. A. Swartzlander, T.J. Coutts, S. Naseem and T.P. Massopust, Thin Solid Films, 138, 65 (1986).

14. K.J. Bachmann, H. Schreiber, Jr., W.R. Sinclair, P.H. Schmidt, F.A. Thiel, E.G. Spencer, G. Pasteur, W.L. Feldmann, and K.S. Sree Harsha, J. Appl. Phys. **50**, 3441 (1979).

15. T.J. Coutts, S. Naseem and R.K. Ahrenkiel, Proceedings 6th European Communities Photovoltaic Solar Energy Conference, London, (1985), D. Reidel Publishing Co., pp. 174-178.

16. D.J. Olego, R. Schachter, M. Viscogliosi and L.A. Bunz, Appl. Phys. Lett., 49, 719 (1986).

Table I. Summary of parameters of solar cells prepared using rf sputtering.[a]

Supplier	Mining and Chemical Products ($3x10^{15}$ cm^{-3})				Crysta-Comm, Inc. ($3x10^{16}$ cm^{-3})			
Cell Ref.	rf1	rf2	rf3	rf4	rf5	rf6	rf7	rf8
LPPE (min)	0	15	30	60	0	15	30	60
J_{sc} (mA cm^{-2})	24.0	25.9	26.3	27.2	23.3	24.5	25.6	24.9
V_{oc} (mV)	746	761	760	785	760	756	759	765
FF (%)	69.3	65.4	66.7	72.2	66.2	73.9	73.7	61.1
η (%)	12.4	12.9	13.3	15.4	11.7	13.7	14.3	11.6

[a]All the cells whose properties are summarized in the table were made by rf sputter deposition of ITO onto the InP substrates immediately after exposure of the latter to the low power plasma. Their characteristics were measured at SERI at 28°C, using a standard spectrum, atmosphere, and other experimental conditions. There was an interval of approximately one month between their fabrication and characterization.

Table II. Summary of parameters of solar cells prepared using ion-beam sputtering.[a]

Supplier	Mining and Chemical Products ($3x10^{15}$ cm^{-3})				Crysta-Comm, Inc. ($3x10^{-16}$ cm^{-3})			
Cell Ref.	IB1	IB2[b]	IB3	IB4	IB5	IB6	IB7	IB8
LPPE (min)	0	15	30	60	0	15	30	60
J_{sc} (mA cm^{-2})	27.7	23.5	26.5	26.0	27.1	26.3	26.1	25.8
V_{oc} (mV)	674	676	773	768	693	758	765	756
FF (%)	65.4	67.1	64.4	65.1	63.9	69.8	64.9	70.8
η (%)	12.2	10.7	13.2	13.0	12.0	13.9	13.0	13.8

[a]These cells were prepared on substrates which had been given the LPPE treatment several weeks before the ITO was deposited by ion-beam sputtering. Therefore, it is possible that a surface oxide may have formed, thus increasing the series resistance and decreasing the fill-factor.

[b]Cell IB2 was accidentally exposed to the ion-beam for several seconds before deposition was begun; it cannot therefore be regarded as one of the family of cells.

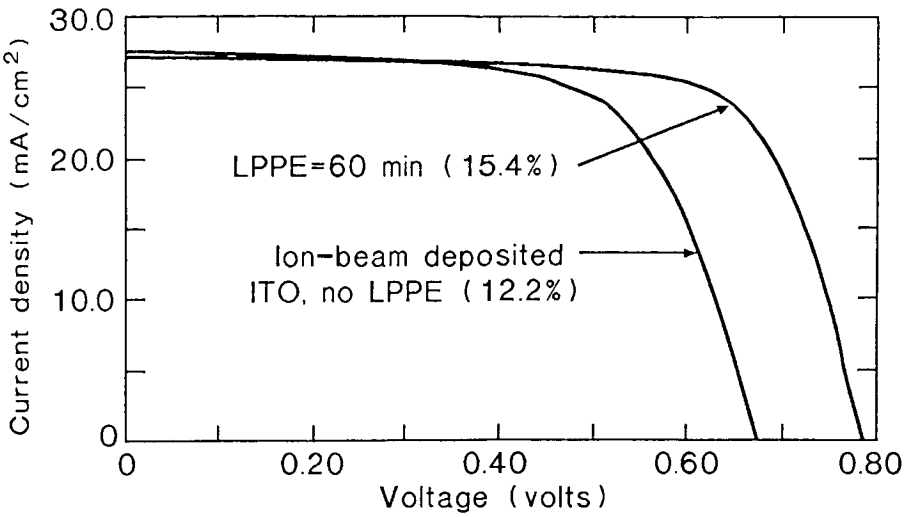

1. - Current/Voltage characteristics of cells 1B1 and rf4. Note that the use of the low-power plasma exposure resulted in a considerably larger V_{oc}.

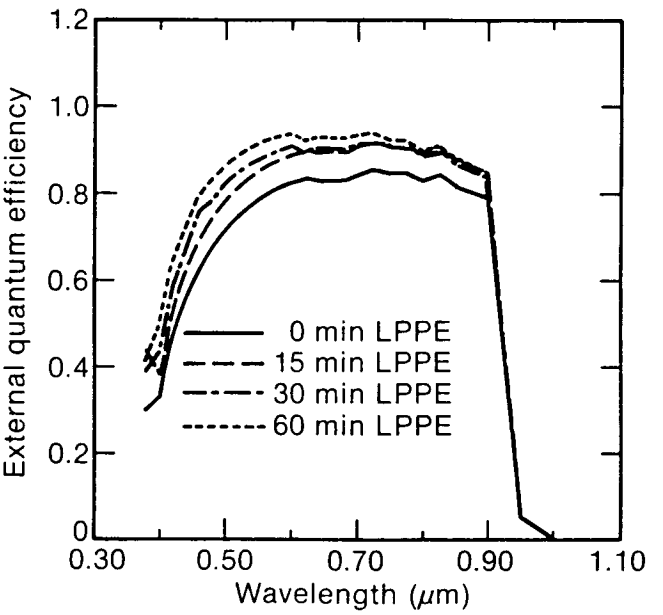

2. - External quantum efficiencies of cells rf1-4. Note the systematic improvement with the increasing duration of the low-power plasma exposure.

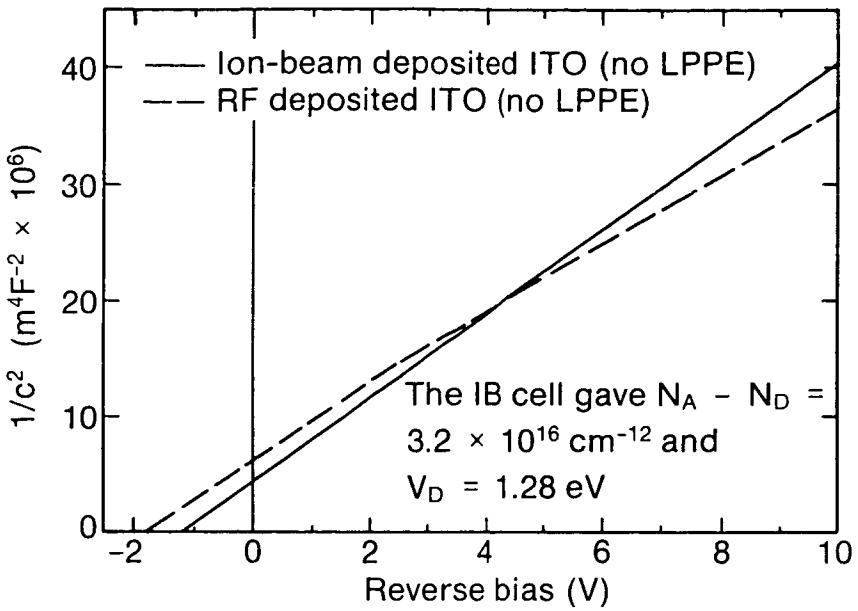

3. - Mott-Schottky plot for cells rf1 and IB1. Even without the plasma exposure, cell rf1 exhibited non-linearity which, it is believed, is indicative of homojunction formations.

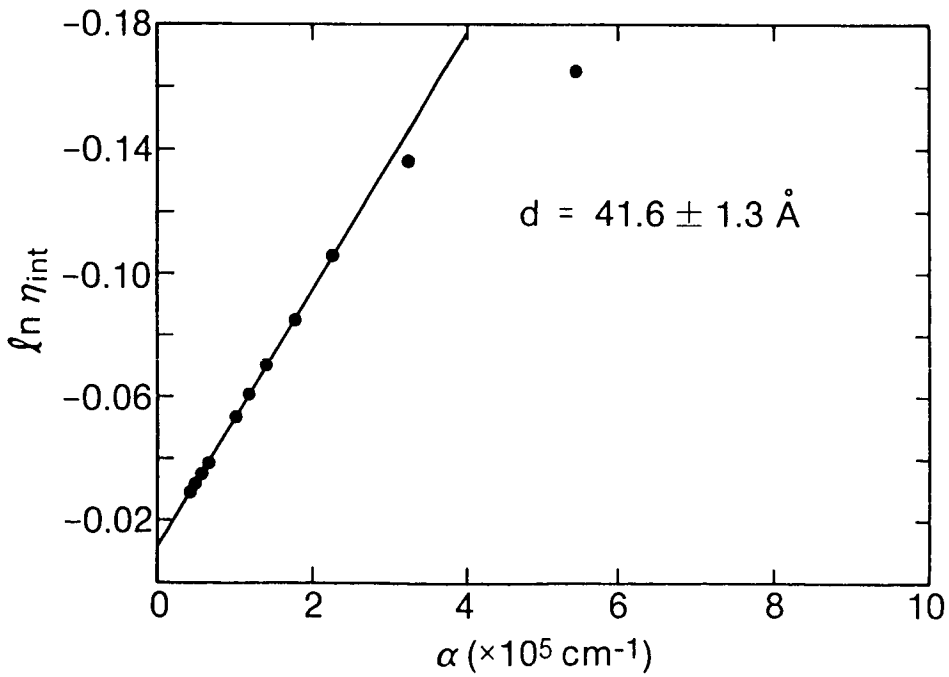

4. - "Dead-layer" plot for a typical cell.

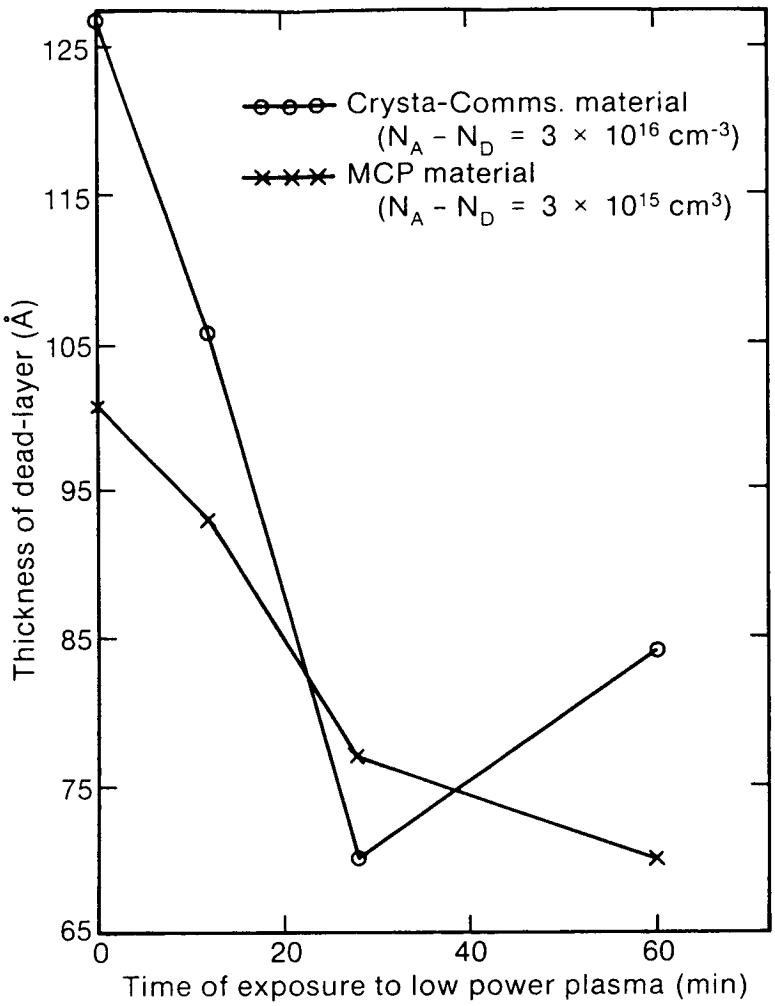

5. - Variation of dead-layer thickness as a function of the duration of the low-power plasma, for two values of $|N_A - N_D|$.

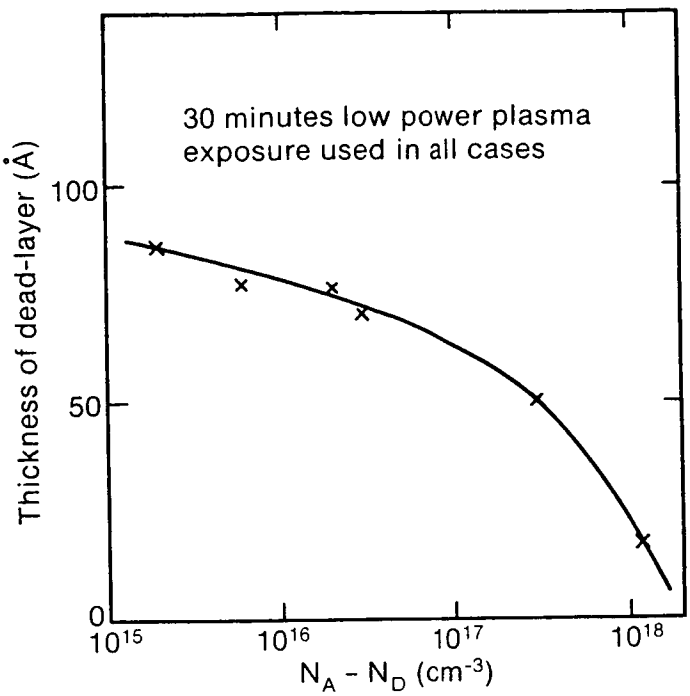

6. - Variation of dead-layer thickness as a function of substrate impurity concentration for a fixed duration plasma exposure.

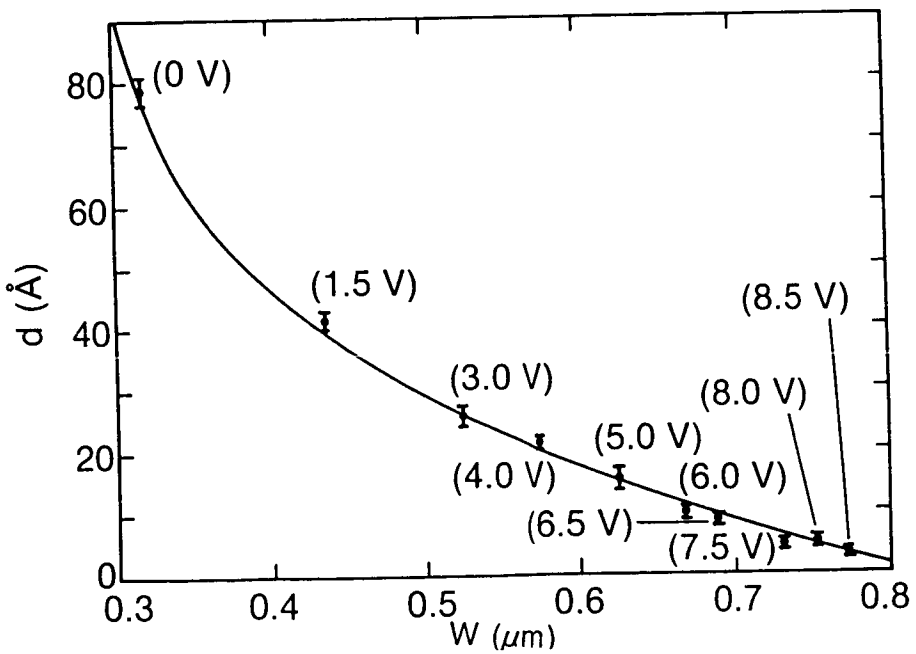

7. - Variation of dead-layer thickness as a function of the total width of the space charge region. It is believed that this result, for one of the rf series cells, indicates an expansion of the space charge toward the ITO/InP interface as well as into the p-InP substrate. This supports the buried homojunction model.